Termination and Verwey transition of the (111) surface of magnetite studied by scanning tunneling microscopy and first-principles calculations

Tomoko K. Shimizu,[1] Jaehoon Jung,[1,2] Hiroyuki S. Kato,[3] Yousoo Kim,[1,*,†] and Maki Kawai[2,*,‡]
[1]*Surface and Interface Science Laboratory, Advanced Science Institute, RIKEN, 2-1 Hirosawa, Wako, Saitama 351-0198, Japan*
[2]*Department of Advanced Materials Science, The University of Tokyo, 5-1-5 Kashiwanoha, Kashiwa, Chiba 277-8561, Japan*
[3]*Surface Chemistry Laboratory, Advanced Science Institute, RIKEN, 2-1 Hirosawa, Wako, Saitama 351-0198, Japan*
(Received 15 April 2010; revised manuscript received 2 June 2010; published 21 June 2010)

Scanning tunneling microscopy and scanning tunneling spectroscopy combined with first-principles calculations have been applied to investigate the (111) surface of a naturally grown Fe_3O_4 single crystal. The commonly observed surface is determined as a layer of Fe cations at tetrahedral sites, known as the Fe_{tet1} termination. A surface terminated with Fe cations at octahedral sites, another proposed termination in previous studies, is found only when the surface was prepared under oxygen-poor conditions. Scanning tunneling spectra at room temperature and at 77 K indicate that the (111) surface undergoes a metal-insulator transition.

DOI: 10.1103/PhysRevB.81.235429 PACS number(s): 68.37.Ef, 68.35.Rh

I. INTRODUCTION

The atomic-scale investigation of surface structures and electronic states of oxides with complex bulk structures presents a significant challenge due to the fact that such oxides may have several possible terminations along a particular crystal direction. It is crucial to determine the most energetically stable surface termination because surface properties depend greatly on atomic composition and structure including defects, impurities, and adsorbates that are commonly present on surfaces. Slight differences in sample preparation often bring about different phases, which make it difficult to determine surface termination.

The (111) surface of magnetite Fe_3O_4 offers a good example of this challenge. Magnetite is one of three naturally occurring iron oxides and has attracted much attention because of its ferrimagnetic properties, theoretically predicted half metallicity,[1,2] and unique phase transition, known as the Verwey transition.[3] As the temperature decreases, at the Verwey transition temperature of ~120 K, conductivity drops by two orders of magnitude and bulk structure transforms from cubic to monoclinic. At room temperature (RT), the structure is inverse spinel, where O^{2-} anions form a face-centered-cubic (fcc) sublattice and Fe^{2+} and Fe^{3+} cations locate at interstitial sites with tetrahedral and octahedral coordination; further details may be found in Ref. 4.

The (100) surface is fairly well understood. There are only two types of stable planes along the [100] direction: "*A*" that contains only tetrahedrally coordinated Fe cations and "*B*" that consists of oxygen anions and octahedrally coordinated Fe cations. Recent density-functional theory (DFT),[5,6] spin-polarized photoelectron spectroscopy (SP-PES),[7] scanning tunneling microscopy (STM),[7–9] and low-energy electron diffraction[10] (LEED) all showed consistent results: the (100) surface is terminated by *B* planes with Jahn-Teller distortion.

In contrast, stable termination of the (111) surface is still in debate. The (111) surface of magnetite has been studied using various surface science techniques because of its importance in geochemistry, device application, and catalysis.[4] There are six atomic planes along the [111] direction, which can be written as, using notations used in previous studies,[11–16] Fe_{tet1}, O_1, Fe_{oct1}, O_2, Fe_{tet2}, and Fe_{oct2}. Adsorption and reaction of molecules on $Fe_3O_4(111)$ have also been studied, but with the assumption of a certain type of termination.[17–23] These results may have to be revisited when the stable surface termination is reliably identified.

It has been suggested both theoretically and experimentally that either Fe_{tet1} or Fe_{oct2} is the stable termination. Fe_{tet1} is a surface terminated by a layer of Fe^{3+} cations at tetrahedral sites and Fe_{oct2} is a surface where the next layer of Fe cations at octahedral sites is added to the Fe_{tet1} termination. Several groups have grown thin films on Pt(111) in a controlled manner. The resultant $Fe_3O_4(111)$ surfaces routinely exhibit identical surface structures, which appear in RT STM images as a hexagonal lattice with approximately 0.6 nm periodicity.[4,12] RT STM on synthetic single crystals exhibited exactly the same surface structures as thin-film samples.[13,24] This surface is referred to as the "regular termination" in Refs. 13 and 24, and we hereinafter use the same terminology. Based on the LEED *I-V* measurements,[11,12,25] the regular termination has been suggested to be the Fe_{tet1} termination with strong relaxation along the [111] direction. In contrast, another group has found evidence supporting the Fe_{oct2} termination by temperature programmed desorption, infrared reflection absorption spectroscopy, and high-resolution electron energy loss spectroscopy after adsorbing CO molecules.[14] Structures that are attributed to FeO(111) have also been observed on thin film[12] and synthetic single crystal,[13] but only when the surface was prepared in oxygen-poor conditions.

In addition to the hexagonal and FeO(111)-like structures, a honeycomb structure has been found using a naturally grown single crystal.[26,27] The reason for its appearance seems more related to the high annealing temperature than the quality of the crystal.[14] The authors determined the types of termination based on the positions of protrusions and apparent step heights in STM images.[26,27] Their conclusion was that the hexagonal lattice corresponds to 1/4 monolayer of O that caps Fe_{oct1} trimer, and the area showing the honeycomb structure corresponds to the Fe_{oct2} termination.[27] The same group later performed STM studies of the same surface, but with adsorption of molecules.[28] The STM images prior to adsorption of molecules showed two different types of hex-

agonal lattice regions instead of one. By investigating the adsorption preferences of molecules on different regions, they proposed a new interpretation: the region exhibiting the honeycomb structure is the Fe_{oct2} termination with oxygen atoms on top of each Fe_{oct2} site; two types of hexagonal lattice regions are the Fe_{tet1} termination and that with oxygen atoms on top of each Fe_{tet1} site.

Theoretical works have not reached consensus on this issue either, although they all predict that iron termination is more stable than oxygen termination. The first report by Ahdjoudj *et al.* used *ab initio* periodic Hartree-Fock calculation, which suggested Fe_{oct2} termination.[29] Grillo *et al.* questioned its validity because "Hartree-Fock bulk band structure did not reproduce the known antiferromagnetic alignment of magnetic moments within the tetrahedral and octahedral sublattices." Instead, they proposed the Fe_{tet1} termination based on DFT with generalized gradient approximation (GGA) $+U$ method.[16] Zhu *et al.* predicted that the Fe_{oct2} termination is energetically favored from their DFT using local density approximation (LDA)$+U$ approach. In the presence of vacancies of the outermost iron layer, however, the Fe_{tet1} termination becomes more stable.[15]

Here, we report an experimental STM study of $Fe_3O_4(111)$ at RT (cubic phase) and at 77 K (monoclinic phase), above and below the Verwey transition temperature. STM image simulations based on the first-principles calculations have also been carried out for the cubic phase. Combining these methods, we were able to identify the routinely observed surface, or regular termination, as the Fe_{tet1} termination. In contrast, the Fe_{oct2} termination appeared only when the sample was prepared under oxygen-poor conditions. In addition, scanning tunneling spectra supported the position that $Fe_3O_4(111)$ undergoes the metal-insulator transition.

II. EXPERIMENTAL

Experiments were performed in two ultrahigh vacuum (UHV) systems. A low-temperature STM (Omicron LT-STM) was employed for STM imaging and scanning tunneling spectroscopy (STS) at 77 K and RT. STS was acquired using a standard lock-in technique with a bias modulation of 50 mV and 797 Hz while opening the feedback loop. LEED was performed in the preparation chamber before STM. Another UHV system was used for x-ray photoelectron spectroscopy (XPS). STM was also performed at RT (Omicron VT-STM) after XPS measurements to confirm the surface termination being the same as that prepared in the LT-STM system.

We used a naturally grown $Fe_3O_4(111)$ single crystal purchased from MaTeck GmbH for all of the experiments described here. It was first degassed in UHV by gradually increasing the temperature up to 770 K. It was then cleaned with a few cycles of Ar^+ ion sputtering (800 eV) for 10 min and annealing at 850 K in UHV for 10 min. The annealing temperature was chosen based on the phase diagram (temperature vs partial pressure of O_2) provided in Ref. 30 in order to prevent the reduction in the surface. After undergoing this cleaning procedure, LEED exhibited the same patterns as those observed in previous studies.[11–13,25,26] The crystal gradually lost oxygen while under UHV for several months. Every time we found an oxygen deficient area in the STM images (see Sec. IV A), we cleaned the sample again with cycles of Ar^+ ion sputtering and annealing in partial O_2 pressure of 1×10^{-7} mbar at 850 K, which resulted in a surface with regular termination.

For identification of adsorbed species, we introduced milli-Q water that was degassed with repeated cycles of freezing, pumping, and thawing into the UHV chamber through a leak valve. The sample was placed right next to the dosing tube attached to the valve. The sample temperature during the adsorption was RT.

III. THEORETICAL

First-principles calculations using GGA and GGA$+U$ methods were carried out in order to investigate the interactions of Fe_{tet1} and Fe_{oct2} terminated $Fe_3O_4(111)$ surfaces with the tunneling electron. The Perdew-Wang exchange-correlation functional[31,32] was used and the inner electrons were replaced with projector augmented wave pseudopotentials,[33,34] expanded in a basis set of plane waves up to a cutoff energy of 460 eV. We used the on-site Coulomb (U) and exchange (J) parameters of 5 and 1 eV, respectively, which were used successfully to reveal the electronic and magnetic properties of the low temperature monoclinic ($P2/c$) crystal structure.[35] A Gaussian smearing ($\sigma=0.05$ eV) of the eigenstates was used to improve the convergence.

The (1×1) surface supercells were employed to describe the Fe_{tet1} and Fe_{oct2} terminated $Fe_3O_4(111)$ surfaces [Fig. 1(a)]. The calculated lattice constants are 8.37 and 8.46 Å using GGA and GGA$+U$, respectively, which agree with the experimental value of 8.3956 Å.[36,37] Figure 1(b) shows the slab model used in the calculation, with periodic separations of about 18 Å. During the ionic relaxations, the bottom two oxygen (O_1 and O_2), two Fe_{oct} (Fe_{oct1} and Fe_{oct2}), and two Fe_{tet} (Fe_{tet1} and Fe_{tet2}) layers were fixed at their bulk values of the cubic ($Fd\bar{3}m$) phase structure. Calculated layer spacing agrees well with experimentally obtained values using LEED I-V.[11] Ionic relaxations were performed until the atomic force was less than 0.01 eV/Å. A $9\times9\times1$ Monkhorst-Pack grid was used for k-point sampling of the Brillouin zone. STM image simulations were performed for Fe_{tet1} and Fe_{oct2} terminated $Fe_3O_4(111)$ surfaces using the Tersoff-Hamann approach,[38] with experimental biases and at a height of 4 Å above the metal surface. The Vienna Ab-initio Simulation Package (VASP) code[39,40] was used in the calculation.

IV. RESULTS AND DISCUSSION

A. Surface structure of the regular termination

When magnetite is cooled below the Verwey transition temperature $T_v\sim120$ K, the crystal experiences a structural phase transition. We find protrusions that are hexagonally arranged with approximately 0.6 nm separation in STM images both at RT and 77 K [Fig. 2(a)], which is an identical structure to those observed in earlier studies using synthetic

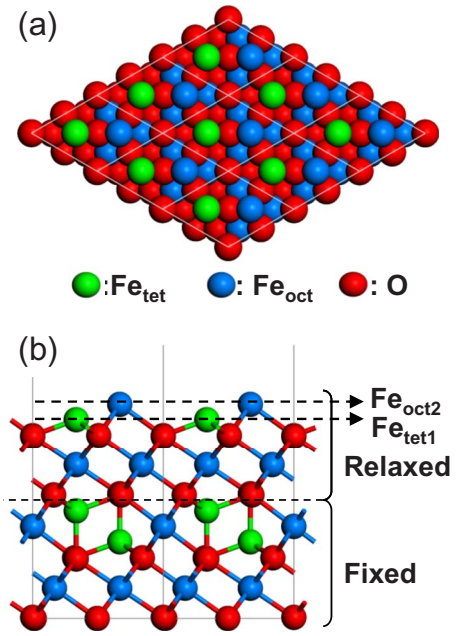

FIG. 1. (Color online) Schematic of atomic arrangement of the $Fe_3O_4(111)$ surface in cubic phase used in the calculations. (a) Top view and (b) side view for the Fe_{oct2} termination are shown. The Fe_{tet1} termination can be constructed just by removing the last Fe_{oct2} layer from the schematics. Five outermost atomic layers (Fe_{oct2}, Fe_{tet1}, O_1, Fe_{oct1}, and O_2) were relaxed to obtain a stable structure.

single crystals,[13,24] natural single crystals,[26–28] and thin films on Pt(111).[4,11,12,14,41] This may indicate that the stronger electron-phonon coupling expected at low-temperature phase[42] does not significantly affect the structure of the (111) surface. However, the surface might experience changes that are too small to be confirmed by STM. The changes in three lattice constants and an angle in the bulk are less than 2 pm and 0.25°.[43] These yield only 1–2 pm difference in the distance between protrusions on the (111) surface. The absence or very small degree of reconstruction is in contrast to the (100) surface, for which reconstruction is observed even at RT.[7–9] Based on DFT calculation, Łodziana suggested that the reconstruction is related to the orbital ordering which opens the energy gap.[6]

In most cases, we found terraces of only this type of termination with an identical step height of 0.48 ± 0.02 nm throughout the surface explored. This measured height agrees well with a half of the unit cell along the [111] direction of the inverse spinel structure. The height is identical for RT and 77 K within experimental error, which again indicates that the structural transformation at T_v is very small. Protrusions of the lattice on the upper terrace are found to be located at one of the two threefold hollow sites (either hcp hollow or fcc hollow) of the lattice on the lower terrace (STM image not shown), which is consistent with the atomic arrangement of the bulk Fe_3O_4.

A few distinct features that are different from the protrusions forming the hexagonal lattice are visible on the surface. In Fig. 2(a), almost all such features appear as depressions. More detailed pictures of these features are shown in Figs. 2(b) and 2(c). The area contains three features that appear

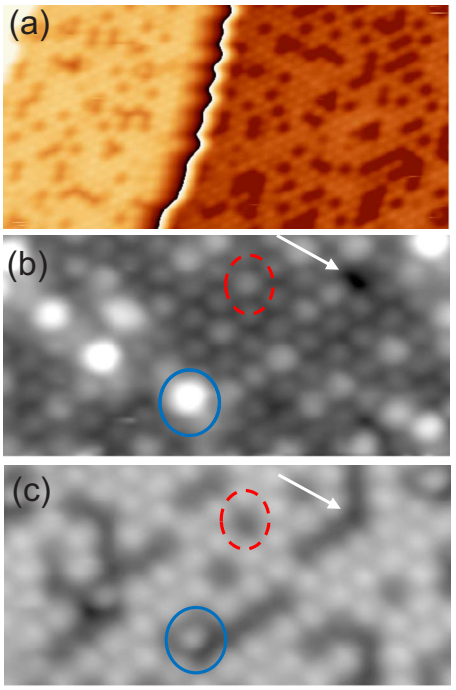

FIG. 2. (Color online) STM images of the regular termination of the $Fe_3O_4(111)$ surface acquired at 77 K. (a) Large-scale image (20×10 nm^2). Step height was measured to be ~480 pm, corresponding to the half the basis vector along the c axis in the inverse spinel structure. Tunneling parameters are $V_{sample} = -2.1$ V and $I_t = 0.4$ nA. (b) and (c) Smaller-scale images (10×5 nm^2) acquired with different bias voltages: (b) $V_{sample} = +4$ V and $I_t = 50$ pA; (c) $V_{sample} = -4$ V and $I_t = 50$ pA. Three types of defects are marked in the images. White arrows indicate a vacancy of the protrusion forming the hexagonal lattice or Fe_{tet1} vacancy; red circled (broken line) and blue circled (solid line) sites are named as P1 and P2 species, respectively.

differently with +4 and −4 V. One type marked by white arrows, which was small in number, is attributed to the vacancy of the Fe_{tet1} atom because it appears as depressions regardless of the tunneling parameters. The assignment agrees with previous studies.[4,12,41] The second type marked by broken red circles (P1) and the third type marked by solid blue circles (P2) can be considered as water-related species such as OH and H arising from dissociative adsorption of residual water. This interpretation is based on observations. We first excluded the possibility of metal contaminants resulting from the natural growth using XPS measurements. The spectra revealed no element except Fe and O within the detection limit. We then intentionally introduced water vapor to the UHV chamber while the sample was kept at RT and observed increases in the numbers of both P1 and P2 species. Similar species found on thin-film Fe_3O_4 were also attributed to the dissociated water since they appeared only when the sample had been kept under UHV for a few hours.[41] Identities of P1 and P2 species will be explored in more detail in the future using both experimental and theoretical approaches.

After keeping the sample in UHV for long time, the surface changed as shown in Fig. 3. We recovered the surface by annealing the crystal at 850 K in an O_2 atmosphere

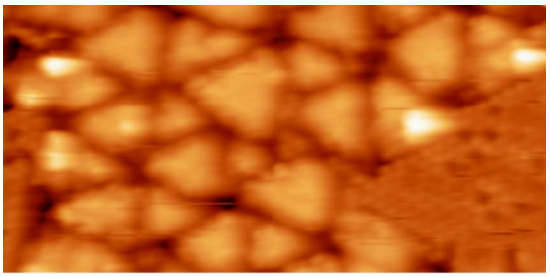

FIG. 3. (Color online) STM image (20×10 nm^2) of oxygen deficient area of the $Fe_3O_4(111)$ surface acquired at 77 K, showing a mixture of a triangular-shaped superstructure and the regular termination. Tunneling parameters are $V_{sample}=-3.0$ V and $I_t=0.2$ nA.

(10^{-7} mbar), which indicates that the new structure appeared because of the surface reduction in an oxygen-poor environment. Thus, the triangular superstructure found here can be considered the same as that observed in Refs. 12, 13, and 27.

B. Verwey transition on the (111) surface

Figure 4(a) shows a typical STS measured at a protrusion forming the hexagonal lattice at 77 K. The inset is another spectrum zoomed into the range between −0.5 and +0.5 V. The energy gap is clearly seen at the Fermi level, indicating that the (111) surface is not in the metallic phase at 77 K. Figure 4(b) shows an *I-V* curve and an STS measured at RT within an area of the hexagonal lattice without defects or adsorbates. The spectra show metallic behavior, suggesting that the (111) surface undergoes the metal-insulator transition between 77 K and RT.

Our observation of the gap closing at RT is inconsistent with a report by Jordan *et al.*[44] They found an energy gap of ~200 meV both at RT and at 95 K in their numerically derived $(dI/dV)/(I/V)$ curve from STM *I-V* measurements, from which they suggested that the surface Verwey transition could be described as a semiconductor-semiconductor transition. We suspect that their spectra might be averaged over the surface with defects or adsorbates. At 77 K, we indeed found a larger energy gap in STS taken right above adsorbates on the (111) surface as shown in Fig. 4(c). On the other hand, the existence of electronic states at the Fermi level has been confirmed by SP-PES on (111) thin films at RT.[45,46] Our calculated projected density of states (not shown) also exhibits nonzero DOS at the Fermi level both on Fe_{tet1} and Fe_{oct2} terminated surfaces in the cubic phase.

C. Identification of surface termination

When the surface still contained a small portion of oxygen deficient area even after a cleaning cycle using annealing in O_2 atmosphere, we also found another type of surface structure right next to the region of the regular termination. Figure 5 shows STM images containing such an area. Region A corresponds to the regular termination discussed in the previous sections. With all tips used in these experiments it appears as a hexagonal lattice within the bias range from −4 to +4 V. A new region marked as B, in contrast, appears

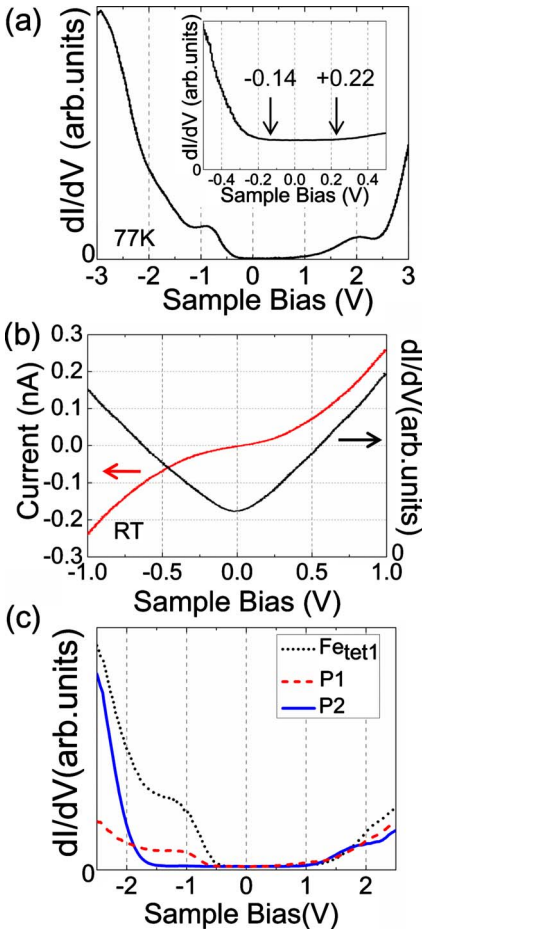

FIG. 4. (Color online) (a) STS obtained on the regular termination at 77 K. Inset: another spectrum that shows the energy gap region in detail. (b) Current-voltage (*I-V*) curve (left y-axis) and STS (right y-axis) obtained at RT on the regular termination. (c) Site-dependent STS obtained on a protrusion forming the hexagonal lattice or Fe_{tet1} site (black dotted line), P1 (red broken line), and P2 species (blue solid line).

either as a honeycomb structure [Figs. 5(a) and 5(c)] or as a hexagonal lattice [Figs. 5(b) and 5(d)] depending on the bias [comparison of Figs. 5(a) and 5(b)] and the tip condition [comparison of Figs. 5(c) and 5(d)]. Sites of protrusions in region A are found to correspond to three of six protrusions forming the honeycomb structure in region B [Fig. 5(a)], but do not correspond to the sites of protrusions in the hexagonal lattice in region B [Fig. 5(b)]. Coexistence of such surface regions has been confirmed also at RT by Lennie *et al.*[26]

The appearance of different surface termination may be explained by the thermodynamic calculation by Grillo *et al.*,[16] who suggested that although the most stable termination is the Fe_{tet1} termination, the Fe_{oct2} termination may still appear under oxygen-poor conditions. Their calculations and our observations are consistent. In region A, the bright protrusions correspond to the Fe_{tet1} sites, while in the images of region B that appear as a hexagonal lattice, the bright protrusions correspond to the Fe_{oct2} sites. In the images of region B that appear as the honeycomb structure, both Fe_{tet1} and Fe_{oct2} sites appear as bright spots.

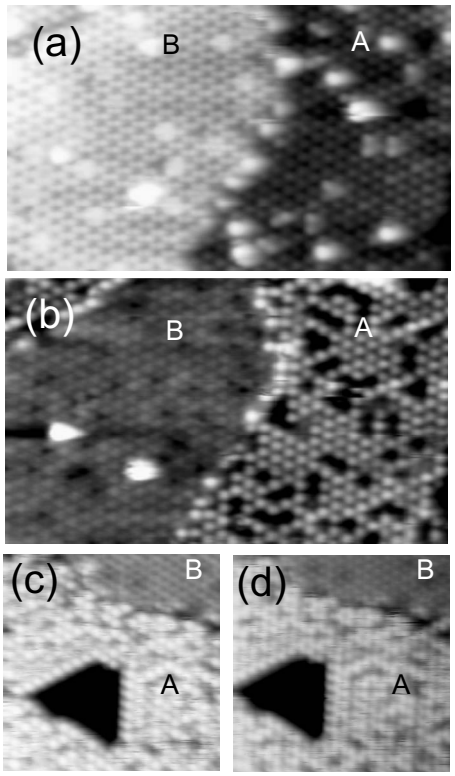

FIG. 5. STM images [(a) and (b) 9×15 nm^2; (c) and (d) 10×10 nm^2] showing bias and tip dependences of the appearances of two regions acquired at 77 K. Region A corresponds to the regular termination. Appearance of region B, either honeycomb or hexagonal lattice, depends both on the [(a) and (b)] bias and [(c) and (d)] tip conditions. Tunneling parameters (a) $V_{sample}=+2.0$ V and $I_t=0.2$ nA; (b) $V_{sample}=-2.0$ V and $I_t=0.2$ nA; (c) and (d) $V_{sample}=-1.0$ V and $I_t=0.2$ nA.

To verify this possible correlation, we performed STM simulations of surfaces terminated by the Fe_{tet1} and Fe_{oct2} layers for the cubic phase. Figure 6 shows the results for the bias voltages at ±2 V. For the Fe_{tet1} termination, protrusions at the Fe_{tet1} sites (marked by blue triangles) form a hexagonal lattice at both bias polarities. In contrast, for the Fe_{oct2} termination, the Fe_{oct2} sites (red circles) appear as bright

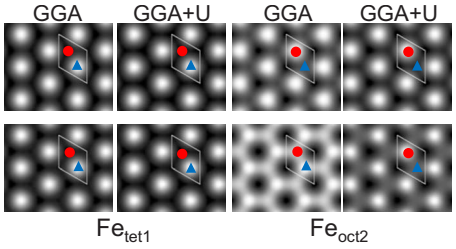

FIG. 6. (Color online) Simulated constant height STM images for the cubic phase using GGA and GGA+U ($U=5$ V and $J=1$ V) methods. Four images on the left correspond to the Fe_{tet1} termination and four images on the right correspond to the Fe_{oct2} termination. Sample bias voltages are set to +2 V (upper row) and −2 V (lower row). Rhombus in each image corresponds to the unit cell. Blue triangles and red circles indicate the Fe_{tet1} and Fe_{oct2} sites, respectively.

spots and form a hexagonal lattice at +2 V, but both Fe_{tet1} and Fe_{oct2} sites appear bright resulting in a honeycomb structure at −2 V. There is a slight difference between the results by GGA and GGA+U: the Fe_{tet1} sites in honeycomb structure appear brighter than the Fe_{oct2} sites by GGA while opposite contrast is found by GGA+U. The simulations qualitatively agree well with the experimental observation, but only under certain tip conditions [e.g., the tip used to acquire Fig. 5(c)]. Bias dependence obtained by the calculation does not agree with some of our experimental images at 77 K [e.g., Figs. 5(a), 5(b), and 5(d)] and RT observations shown in Ref. 26 (honeycomb at +2 V and hexagonal at +1 V). It is not surprising that the calculated bias dependence is different (sometimes opposite) from the experimental results because the simple Tersoff-Hamann approach generates STM images using the local density of states of the surface alone.[38] It does not include the tip density of states that is affected by, for example, chemical composition and geometry. We find that the tips that produce different bias dependence from the simulation often yield clearer and sharper images, which implies chemical modification at the tip apex.

Because throughout all of the experiments the hexagonal lattice was observed on the regular termination (region A), we conclude that it should be the Fe_{tet1} termination. The surface of the Fe_{oct2} termination (region B) appears only after the sample undergoes an oxygen-poor condition. The reason why CO adsorption experiment suggested the Fe_{oct2} termination[14] might be explained if the surface contained both the Fe_{tet1} and Fe_{oct2} terminations. Further consideration and experiments such as STM of CO adsorbed surface will be necessary.

V. CONCLUSION

Two debated issues of the $Fe_3O_4(111)$ surface, the regular termination and the existence of the Verwey transition, were explored by a combined study of STM, STS, and first-principles calculations. The regular surface is terminated by a layer of Fe_{tet1} whereas Fe_{oct2} termination appears only in oxygen-poor conditions. The metal-insulator transition was confirmed by STS even though the structural transformation or surface reconstruction below the Verwey transition temperature is smaller than the length scale distinguishable in STM images.

ACKNOWLEDGMENTS

This work is financially supported in part by Grant-in-Aid for Scientific Research on Priority Areas "Electron Transport through a Linked Molecule in Nano-scale" and Grant-in-Aid for Scientific Research (S) "Single Molecule Spectroscopy Using Probe Microscope" from the Ministry of Education, Culture, Sports, Science, and Technology (MEXT) of Japan. We are grateful for the computational resources of the RIKEN Integrated Cluster of Clusters (RICC) supercomputer system. J.J. kindly acknowledges the International Program Associate (IPA) of RIKEN for financial support. We thank D. Chapmon for carefully reading the manuscript.

*Corresponding author. FAX: +81-48-462-4663.
†ykim@riken.jp
‡maki@k.u-tokyo.ac.jp

[1] A. Yanase and K. Siratori, J. Phys. Soc. Jpn. **53**, 312 (1984).
[2] Z. Zhang and S. Satpathy, Phys. Rev. B **44**, 13319 (1991).
[3] E. J. W. Verwey, Nature (London) **144**, 327 (1939).
[4] W. Weiss and W. Ranke, Prog. Surf. Sci. **70**, 1 (2002).
[5] R. Pentcheva, F. Wendler, H. L. Meyerheim, W. Moritz, N. Jedrecy, and M. Scheffler, Phys. Rev. Lett. **94**, 126101 (2005).
[6] Z. Łodziana, Phys. Rev. Lett. **99**, 206402 (2007).
[7] M. Fonin, R. Pentcheva, Yu. S. Dedkov, M. Sperlich, D. V. Vyalikh, M. Scheffler, U. Rüdiger, and G. Güntherodt, Phys. Rev. B **72**, 104436 (2005).
[8] K. Jordan, G. Mariotto, S. F. Ceballos, S. Murphy, and I. V. Shvetz, J. Magn. Magn. Mater. **290-291**, 1029 (2005).
[9] B. Stanka, W. Hebenstreit, U. Diebold, and S. A. Chambers, Surf. Sci. **448**, 49 (2000).
[10] R. Pentcheva, W. Moritz, J. Rundgren, S. Frank, D. Schrupp, and M. Scheffler, Surf. Sci. **602**, 1299 (2008).
[11] M. Ritter and W. Weiss, Surf. Sci. **432**, 81 (1999).
[12] Sh. K. Shaikhutdinov, M. Ritter, X.-G. Wang, H. Over, and W. Weiss, Phys. Rev. B **60**, 11062 (1999).
[13] M. Paul, M. Sing, R. Claessen, D. Schrupp, and V. A. M. Brabers, Phys. Rev. B **76**, 075412 (2007).
[14] C. Lemire, R. Meyer, V. E. Henrich, Sh. Shaikhutdinov, and H.-J. Freund, Surf. Sci. **572**, 103 (2004).
[15] L. Zhu, K. L. Yao, and Z. L. Liu, Phys. Rev. B **74**, 035409 (2006).
[16] M. E. Grillo, M. W. Finnis, and W. Ranke, Phys. Rev. B **77**, 075407 (2008).
[17] K. T. Rim, J. P. Fitts, T. Müller, K. Adib, N. Camillone III, R. M. Osgood, S. A. Joyce, and G. W. Flynn, Surf. Sci. **541**, 59 (2003).
[18] K. T. Rim, T. Müller, J. P. Fitts, K. Adib, N. Camillone III, R. M. Osgood, E. R. Batista, R. A. Friesner, S. A. Joyce, and G. W. Flynn, J. Phys. Chem. B **108**, 16753 (2004).
[19] Y. Joseph, C. Kuhrs, W. Ranke, M. Ritter, and W. Weiss, Chem. Phys. Lett. **314**, 195 (1999).
[20] Y. Joseph, W. Ranke, and W. Weiss, J. Phys. Chem. B **104**, 3224 (2000).
[21] U. Leist, W. Ranke, and K. Al-Shamery, Phys. Chem. Chem. Phys. **5**, 2435 (2003).
[22] W. Huang and W. Ranke, Surf. Sci. **600**, 793 (2006).
[23] R. S. Cutting, C. A. Muryn, D. J. Vaughan, and G. Thornton, Surf. Sci. **602**, 1155 (2008).
[24] N. Berdunov, S. Murphy, G. Mariotto, and I. V. Shvets, Phys. Rev. B **70**, 085404 (2004).
[25] A. Barbieri, W. Weiss, M. A. Van Hove, and G. A. Somorjai, Surf. Sci. **302**, 259 (1994).
[26] A. R. Lennie, N. G. Condon, F. M. Leibsle, P. W. Murray, G. Thornton, and D. J. Vaughan, Phys. Rev. B **53**, 10244 (1996).
[27] N. G. Condon, F. M. Leibsle, T. Parker, A. R. Lennie, D. J. Vaughan, and G. Thornton, Phys. Rev. B **55**, 15885 (1997).
[28] R. S. Cutting, C. A. Muryn, G. Thornton, and D. J. Vaughan, Geochim. Cosmochim. Acta **70**, 3593 (2006).
[29] J. Ahdjoudj, C. Martinsky, C. Minot, M. A. Van Hove, and G. A. Somorjai, Surf. Sci. **443**, 133 (1999).
[30] G. Ketteler, W. Weiss, W. Ranke, and R. Schlogl, Phys. Chem. Chem. Phys. **3**, 1114 (2001).
[31] J. P. Perdew and Y. Wang, Phys. Rev. B **45**, 13244 (1992).
[32] J. P. Perdew, J. A. Chevary, S. H. Vosko, K. A. Jackson, M. R. Pederson, D. J. Singh, and C. Fiolhais, Phys. Rev. B **46**, 6671 (1992).
[33] G. Kresse and D. Joubert, Phys. Rev. B **59**, 1758 (1999).
[34] P. E. Blöchl, O. Jepsen, and O. K. Andersen, Phys. Rev. B **49**, 16223 (1994).
[35] I. Leonov, A. N. Yaresko, V. N. Antonov, M. A. Korotin, and V. I. Anisimov, Phys. Rev. Lett. **93**, 146404 (2004).
[36] L. W. Finger, R. M. Hazen, and A. M. Hofmeister, Phys. Chem. Miner. **13**, 215 (1986).
[37] H. Okudera K. Kihara, and T. Matsumoto, Acta Crystallogr., Sect. B: Struct. Sci. **52**, 450 (1996).
[38] J. Tersoff and D. R. Hamann, Phys. Rev. Lett. **50**, 1998 (1983).
[39] G. Kresse and J. Hafner, Phys. Rev. B **47**, 558 (1993).
[40] G. Kresse and J. Furthmüller, Phys. Rev. B **54**, 11169 (1996).
[41] Sh. Shaikhutdinov and W. Weiss, J. Mol. Catal. A: Chem. **158**, 129 (2000).
[42] P. Piekarz, K. Parlinski, and A. M. Oleś, Phys. Rev. B **76**, 165124 (2007).
[43] J. P. Wright, J. P. Attfield, and P. G. Radaelli, Phys. Rev. B **66**, 214422 (2002).
[44] K. Jordan, A. Cazacu, G. Manai, S. F. Ceballos, S. Murphy, and I. V. Shvets, Phys. Rev. B **74**, 085416 (2006).
[45] Y. Q. Cai, M. Ritter, W. Weiss, and A. M. Bradshaw, Phys. Rev. B **58**, 5043 (1998).
[46] M. Fonin, Yu. S. Dedkov, R. Pentcheva, U. Rüdiger, and G. Güntherodt, J. Phys.: Condens. Matter **19**, 315217 (2007).